NRL Memorandum Report 3766

Lower-Hybrid-Drift Wave Turbulence in the Distant Magnetotail

J. D. HUBA

Science Applications, Inc.
McLean, Va. 22101

N. T. GLADD and K. PAPADOPOULOS

Plasma Physics Division

May 1978

NAVAL RESEARCH LABORATORY
Washington, D.C.

SECURITY CLASSIFICATION OF THIS PAGE (When Data Entered)

REPORT DOCUMENTATION PAGE		READ INSTRUCTIONS BEFORE COMPLETING FORM
1. REPORT NUMBER NRL Memorandum Report 3766	2. GOVT ACCESSION NO.	3. RECIPIENT'S CATALOG NUMBER
4. TITLE (and Subtitle) LOWER-HYBRID-DRIFT WAVE TURBULENCE IN THE DISTANT MAGNETOTAIL		5. TYPE OF REPORT & PERIOD COVERED Interim report on a continuing NRL problem. 6. PERFORMING ORG. REPORT NUMBER
7. AUTHOR(s) J. D. Huba, SAI, N. T. Gladd and K. Papadopoulos		8. CONTRACT OR GRANT NUMBER(s)
9. PERFORMING ORGANIZATION NAME AND ADDRESS Naval Research Laboratory Washington, D.C. 20375		10. PROGRAM ELEMENT, PROJECT, TASK AREA & WORK UNIT NUMBERS NRL Problem A03-16B ONR - RR033-02-42 (Continues)
11. CONTROLLING OFFICE NAME AND ADDRESS Office of Naval Research, Arlington, Virginia 22217 and National Aeronautics & Space Administration, Washington, D. C. 20546		12. REPORT DATE May 1978 13. NUMBER OF PAGES 52
14. MONITORING AGENCY NAME & ADDRESS(if different from Controlling Office)		15. SECURITY CLASS. (of this report) UNCLASSIFIED 15a. DECLASSIFICATION/DOWNGRADING SCHEDULE
16. DISTRIBUTION STATEMENT (of this Report) Approved for public release; distribution unlimited.		
17. DISTRIBUTION STATEMENT (of the abstract entered in Block 20, if different from Report)		
18. SUPPLEMENTARY NOTES This research was sponsored by ONR Project No. RR033-02-42 and NASA Project No. W-14,365.		
19. KEY WORDS (Continue on reverse side if necessary and identify by block number) Reconnection Fireballs Lower hybrid waves Magnetotail		

20. ABSTRACT (Continue on reverse side if necessary and identify by block number)

Recent satellite observations of electrostatic and magnetic noise in the distant magnetotail (Gurnett et al., 1976) can be explained by the excitation of the lower-hybrid-drift instability. In particular it is shown that (1) existence conditions for the lower-hybrid-drift instability are met, (2) the observed frequency spectra and polarization are in good agreement with the predictions of linear theory, and (3) the observed amplitudes of fluctuations are consistent with the nonlinear theory of this mode. Moreover, the observation of this instability suggests that the anomalous transport properties associated with these waves, which are important in many (Continues)

DD FORM 1 JAN 73 1473 EDITION OF 1 NOV 65 IS OBSOLETE
S/N 0102-014-6601

SECURITY CLASSIFICATION OF THIS PAGE (When Data Entered)

10. Program Element, Project, Task Area & Work Unit Numbers (Continued)

NRL Problem A03-31, NASA-W-14,365

20. Abstract (Continued)

laboratory devices, may play a crucial role in the macroscopic evolution of magnetotail processes such as field line merging, tearing instabilities or "fireballs."

CONTENTS

LOWER-HYBRID-DRIFT WAVE TURBULENCE IN THE DISTANT MAGNETOTAIL

I. Introduction

An important aspect of magnetospheric physics is understanding the abundant processes associated with microscopic plasma turbulence. Some of these turbulent microscopic processes result in anomalous plasma transport properties (i.e., not explainable in terms of classical Coulomb collisions) and hence, greatly influence the macroscopic behavior of the magnetospheric plasma. Many of the most dramatic phenomena in the magnetosphere [e.g., magnetic field line reconnection, magnetic substorms, aurorae] involve turbulent microscopic plasma phenomena in an integral fashion.

We recently proposed (Huba et al., 1977) that the lower-hybrid-drift instability (Krall and Liewer, 1971), an instability of considerable importance in several magnetic fusion confinement systems (e.g., Davidson et al., 1976; Commisso and Griem, 1977), would be operative over large regions of the magnetotail and furthermore, may play a significant role in the development of field line reconnection as a source of anomalous resistivity. In this paper we demonstrate that recent experimental measurements of magnetotail turbulence support our theoretical prediction that the lower-hybrid-drift instability is active in the magnetotail. However, the one-dimensional, laminar equilibrium used in Huba et al. (1977) is overly simplistic in modelling the plasma sheet since experimental observations indicate it is generally a turbulent medium (Frank et al., 1976; Coroniti et al., 1977). Rather, localized spatial gradients within a much broader plasma sheet are considered to excite lower-hybrid-drift turbulence in the magnetotail.

Gurnett et al. (1976) have made detailed satellite observations of

Note: Manuscript submitted March 23, 1978.

plasma turbulence in the distant magnetotail (23-46 R_E) and have found broad-band electrostatic noise, magnetic noise and electrostatic electron cyclotron noise. The broadband electrostatic turbulence is the most intense and frequently occurring type, and is strongest in the frequency range $\Omega_i \ll \omega \leq \Omega_e$. The turbulence is observed in regions of strong plasma and magnetic field gradients in the plasma sheet, where reconnection and/or tearing modes are believed to exist. The magnetic noise is observed in the same spatial regions and same frequency range as the electrostatic noise, but occurs less frequently. The electrostatic electron cyclotron turbulence is only observed occasionally, tending to occur in very hot regions near the neutral line. Gurnett et al. (1976) suggested that the broadband electrostatic noise could be produced by field aligned currents and that the magnetic noise could be generated by a whistler instability. The electron cyclotron emissions seem to be of the type studied by Fredricks (1971), Young et al. (1973), Ashour-Abdalla and Kennel (1976) and others, and will not be discussed in this paper.

In this paper we examine the experimental observations of Gurnett et al. (1976) in the light of theoretical studies of the lower-hybrid-drift instability, and find strong evidence for the existence of this instability in terms of existence criteria, spectral characteristics and amplitude of fluctuations. Furthermore, our theoretical model explains both the broadband electrostatic noise and the magnetic noise within the context of the lower-hybrid-drift instability.

The lower-hybrid-drift instability (Krall and Liewer, 1971; Davidson and Gladd, 1975; Gladd, 1976; Huba and Wu, 1976; Davidson et al., 1977)

is a cross-field current driven instability which has been found to be an important anomalous transport mechanism in laboratory plasmas (Davidson et al., 1976; Commisso and Griem 1977). The free energy which supports the instability is provided by the cross-field current and inhomogeneities in the plasma and magnetic field. The scale lengths of the inhomogeneities needed to excite the instability can be many mean ion Larmor radii, $L_n \leq (m_i/m_e)^{\frac{1}{4}} r_{Li}$, where L_n is the characteristic scale length of the density inhomogeneity and r_{Li} is the mean ion Larmor radius. For weaker gradients, $(m_i/m_e)^{\frac{1}{2}} < L_n$ $(m_i/m_e)^{\frac{1}{4}}$, the lower-hybrid-drift instability transforms into the drift cyclotron instability (Mikhailovskii and Timofeev, 1963: Freidberg and Gerwin, 1977). The nature of the lower-hybrid-drift instability is twofold. In the presence of strong plasma gradients ($L_n/r_{Li} \leq 1$), it is a fluid instability excited through a coupling of a lower hybrid wave and a drift wave. When plasma inhomogeneities are weak ($(m_e/m_i)^{\frac{1}{4}} > L_n/r_{Li} \geq 1$) it is a kinetic instability driven by a resonance between ions and a drift wave. An important advantage of this instability over other cross-field current driven instabilities (e.g., ion acoustic instability and Buneman instability) is that it can readily be excited for much weaker drift currents and persists in the regime $T_e < T_i$, which is generally believed to be the case in the magnetotail. Moreover, in finite β plasmas, both electrostatic and electromagnetic turbulence is produced by this instability.

We take this opportunity to comment on the fact that although this instability is thought to be important in a number of magnetic fusion confinement systems (e.g., theta pinches, reversed field pinches, mirror machines), it is very difficult to make detailed laboratory measurements of plasma turbulence of the type made by Gurnett et al. (1976) in the magneto-

tail. Therefore, it is interesting to note that the detailed experimental information necessary to decide which of several possible nonlinear mechanisms is most important in saturating the instability and hence, in determining the plasma parametric dependence of the various anomalous transport processes, may well come from measurements of space plasmas.

The scheme of the paper is as follows. In the next section we present the linear and nonlinear theories of the lower-hybrid-drift instability with an emphasis on the fundamental physical processes. In Section III we outline the essential features of the observational results. In Section IV we present a detailed comparison of the theoretical predictions with the observational results. In the final section we discuss possible consequences of the observed turbulence in regard to field line reconnection and tearing instabilities in the magnetotail.

II. Theory

A. Assumptions and Plasma Configuration

The plasma configuration and slab geometry used in the analysis are shown in Fig. 1. The equilibrium magnetic field is $\underline{B} = B(x)\hat{e}_z$. We assume the density and magnetic field vary only in the x direction, and for simplicity, that the temperature is constant. The electrons drift in the y direction with a mean fluid velocity ($m_e \to 0$) $V_{ey} = V_{de}$ where $V_{de} = -(v_e^2/2\Omega_e)\,\partial \ln n/\partial x$ is the electron diamagnetic drift velocity, $n = n_e \approx n_i$ is the density, and $v_\alpha = (2T_\alpha/m_\alpha)^{\frac{1}{2}}$ is the thermal velocity, $\Omega_\alpha = |e_\alpha|B/m_\alpha c$ is the cyclotron frequency, e_α is the charge, T_α is the temperature and m_α is the mass, all of species α. Equilibrium force balance on an ion fluid element in the x direction requires $V_{iy} = V_{di}$ where $V_{di} = (v_i^2/2\Omega_i)\,\partial \ln n/\partial x$ is the ion diamagnetic drift velocity. Moreover, we can relate the ion diamagnetic drift velocity to the scale length of the density gradient through $V_{di}/v_i = \frac{1}{2} r_{Li}/L_n$ where $L_n^{-1} = \partial \ln n/\partial x$. The electrons are assumed to be magnetized while the ions are treated as unmagnetized. This is a reasonable assumption since we are considering waves such that $\Omega_i \ll \omega \ll \Omega_e$ and $kr_{Li} \gg 1$, where $r_{L\alpha} = v_\alpha/\Omega_\alpha$ is the mean Larmor radius of species α. We consider only flute perturbations ($\underset{\sim}{k}\cdot\underset{\sim}{B} = 0$) and assume $k_y^2 \gg k_x^2 \gg (\partial \ln n/\partial x)^2$, $(\partial \ln B/\partial x)^2$ which justifies the use of the local approximation (Krall, 1968). Finally, we assume the plasma is weakly inhomogeneous in the sense that $r_{Le}^2\,(\partial \ln n/\partial x)^2 \ll 1$ and $r_{Le}^2\,(\partial \ln B/\partial x)^2 \ll 1$.

B. Linear Theory

A comprehensive discussion of the linear theory of the lower-hybrid-drift instability has been given by Davidson et al. (1977). We only present the basic results of the theory at this time and refer the reader to Davidson

et al. (1977) for details.

The local equilibrium distribution functions of the electrons and ions are, respectively,

$$F_{eo} = \frac{n(x)}{(\pi v_e^2)^{3/2}} \left[1 - \frac{v_y}{\Omega_e L_n}\right] \exp\left[-v^2/v_e^2\right]$$

and

$$F_{io} = \frac{n(x)}{(\pi v_i^2)^{3/2}} \exp\left[-(v_x^2 + (v_y - V_{di})^2 + v_z^2)/v_i^2\right]$$

where $V_{di} = (v_i^2/2\Omega_i)[\partial \ln n/\partial x]_{x=x_o}$ and the perturbations are assumed to be well localized about $x=x_o$. We emphasize that F_{io} is a valid local equilibrium even when the ion orbits are large (i.e., $r_{Li}/L_n \approx 1$) (Davidson and Gladd, 1977). Following Davidson et al. (1977), the equations which describe the lower-hybrid-drift instability are

$$D_{xx}(\omega,k)\delta\hat{E}_x + D_{xy}(\omega,k)\delta\hat{E}_y = 0 \qquad (1)$$

$$D_{yx}(\omega,k)\delta\hat{E}_x + D_{yy}(\omega,k)\delta\hat{E}_y = 0 \qquad (2)$$

where $\delta\underset{\sim}{E} = \delta\hat{\underset{\sim}{E}} \exp[i(ky-\omega t)]$,

$$D_{xx}(\omega,k) = 1 - \frac{c^2k^2}{\omega^2} - \frac{2\omega_{pe}^2}{\omega^2}\,\Phi_1, \qquad (3)$$

$$D_{xy}(\omega,k) = -D_{yx}(\omega,k) = 2i\,\frac{\omega_{pe}}{\omega}\,\frac{\omega_{pe}}{kv_e}\,\Phi_2, \qquad (4)$$

$$D_{yy}(\omega,k) = 1 + \frac{2\omega_{pi}^2}{k^2v_i^2}\left[1+\xi_i Z(\xi_i)\right] + \frac{2\omega_{pe}^2}{k^2v_e^2}(1-\Phi_3), \qquad (5)$$

$\xi_i = (\omega - kV_{di})/kv_i$, $Z(\xi) = (\pi)^{-\frac{1}{2}} \int_{-\infty}^{\infty} dx\, \exp(-x^2)/(x-\xi)$, and Φ_1, Φ_2 and Φ_3 are defined by

$$\Phi_j = \Lambda \int_0^{\infty} ds^2\, \frac{F_j \exp(-s^2)}{\omega - k\bar{V}_B s^2} \qquad j = 1.2.3, \qquad (6)$$

where $F_1 = (sJ_1(\mu))^2$, $F_2 = sJ_o(\mu)J_1(\mu)$, $F_3 = J_o^2(\mu)$, $\mu = kr_{Le}s$, $s = v_\perp/v_e$, $\Lambda = \omega - kV_{de}$, $\bar{V}_B = -(v_e^2/2\Omega_e)\partial \ell n\, B/\partial x$ and $J_n(\mu)$ is the Bessel function of order n. The fluctuating magnetic field associated with the electromagnetic oscillations is given by

$$\delta\hat{B}_z = -\frac{ck}{\omega}\,\delta\hat{E}_x \tag{7}$$

The dispersion equation can be found from $\det[\underset{\sim}{D}] = D_{xx}D_{yy} - D_{xy}D_{yx} = 0$ which yields

$$D(\omega,k) = \left[1 + \frac{2\omega_{pi}^2}{k^2v_i^2}\,(1 + \xi_i Z(\xi_i)) + \frac{2\omega_{pe}^2}{k^2v_e^2}\,(1-\Phi_3)\right] + \tag{8}$$

$$+ \frac{2\omega_{pe}}{c^2k^2}\,\frac{2\omega_{pe}^2}{k^2v_e^2}\,\Phi_2^2\left(1 + \frac{2\omega_{pe}^2}{c^2k^2}\,\Phi_1\right)^{-1} = 0$$

where we have assumed $\omega^2 \ll c^2k^2$. We emphasize that Eq. (8) is valid for plasmas of arbitrary β $(= 8\pi n(T_e+T_i)/B^2)$, an important consideration in modelling the magnetotail. The first term in Eq. (8) represents the electrostatic contribution to the mode while the second term contains the electromagnetic corrections. Moreover, the ∇B orbit modifications of the electrons are treated properly since they can give rise to important electron-wave resonances (Huba and Wu, 1971).

A qualitative understanding of the lower-hybrid-drift instability can be obtained if we consider only electrostatic oscillations $(\omega_{pe}^2 \ll c^2k^2)$ and cold electrons $(T_e \to 0)$. In this limit Eq. (8) reduces to

$$D(\omega,k) = 1 + \frac{\omega_{pe}^2}{\Omega_e^2} - \frac{2\omega_{pi}^2}{k^2v_i^2}\,\frac{kV_{di}}{\omega} + \frac{2\omega_{pi}^2}{k^2v_i^2}\,(1+\xi_i Z(\xi_i)) = 0 \tag{9}$$

where we have used $V_{di} = -\frac{T_e}{T_i}V_{de}$. Two types of instability can occur depending on the magnitude of the drift velocity. We now examine

each case separately.

1. $V_{di} \gg v_i$ (fluid instability)

We assume $V_{di} \gg v_i$ and $\omega \gg kv_i$ which allows us to make the approximation $Z(\xi) \simeq -1/\xi - 1/2\xi^3$. It is easily shown that Eq. (9) becomes

$$D(\omega,k) = 1 + \frac{\omega_{pe}^2}{\Omega_e^2} - \frac{\omega_{pi}^2}{(\omega-kV_{di})^2} - \frac{2\omega_{pi}^2}{k^2v_i^2}\,\frac{kV_{di}}{\omega} = 0 \qquad (10)$$

which can be rewritten as

$$1 - \frac{(\omega-kV_{di})^2}{\omega_{\ell h}^2}\left(1 - \frac{kV_{di}}{\omega}\,\frac{2\omega_{\ell h}^2}{k^2v_i^2}\right) = 0 \qquad (11)$$

where $\omega_{\ell h} = \omega_{pi}/(1+\omega_{pe}^2/\Omega_e^2)^{\frac{1}{2}}$ is the generalized lower hybrid frequency. Analysis of Eq. (11) indicates that an instability can occur when $\omega - kV_{di} < 0$ with $\omega_r \simeq \gamma \simeq \omega_{\ell h}$ (Krall and Liewer, 1971). In this situation a Doppler shifted lower hybrid wave $(\omega_1 - kV_{di} = \pm\,\omega_{\ell h})$ is coupled to a drift wave $(\omega_2 = kV_{di}(2\omega_{\ell h}^2/k^2v_i^2))$ as shown in Eq. (11).

2. $V_{di} \ll v_i$ (kinetic instability)

In this limit we assume $\omega \ll kv_i$ so that $Z(\xi) \approx i\sqrt{\pi}k/|k|$. We find that Eq. (7) becomes

$$D(\omega,k) = 1 + \frac{\omega_{pe}^2}{\Omega_e^2} - \frac{2\omega_{pi}^2}{k^2v_i^2}\,\frac{kV_{di}}{\omega} + \frac{2\omega_{pi}^2}{k^2v_i^2}\left(1 + \frac{\omega-kV_{di}}{|k|v_i}\,i\sqrt{\pi}\right) = 0. \qquad (12)$$

It readily follows from Eq. (12), that for $\gamma \ll \omega_r$,

$$\omega_r = kV_{di}\,\frac{2\omega_{pi}^2}{k^2v_i^2}\left(1 + \frac{2\omega_{pi}^2}{k^2v_i^2} + \frac{\omega_{pe}^2}{\Omega_e^2}\right)^{-1} \qquad (13)$$

and

$$\gamma = -\sqrt{\pi}\,\frac{\omega_r - kV_{di}}{kv_i}\,\frac{\omega_r^2}{kV_{di}} \qquad (14)$$

Clearly, an instability is possible ($\gamma > 0$) when $\omega_r - kV_{di} < 0$. The instability is produced by ions in resonance with the drift wave (Eq. (13)). Maximizing γ with respect to k, we may easily show that

$$\gamma_M = \frac{\sqrt{2\pi}}{8}\left(\frac{V_{di}}{v_i}\right)^2 \omega_{\ell h} \tag{15}$$

$$\omega_M = \frac{1}{\sqrt{2}}\left(\frac{V_{di}}{v_i}\right)\omega_{\ell h} \tag{16}$$

and $k_M = \sqrt{2}\,\omega_{\ell h}/v_i$ with the subscript M denoting values corresponding to maximum growth. Although it has been assumed that $V_{di}^2 \ll v_i^2$, numerical computations verify that these expressions are in fact accurate up to $V_{di} \sim v_i$.

For parameters typical of the magnetotail, the kinetic instability is likely to dominate since it corresponds to inhomogeneity scale lengths greater than or about the mean ion Larmor radius ($r_{Li}\,\partial \ell n\, n/\partial x \leq 1$). However, in general, the approximations made in deriving Eqs. (12) - (16) are not valid in the magnetotail and a numerical solution of Eq. (8) is required to determine the frequency and growth rate of the wave.

To illustrate the wave characteristics of Eq. (8) for typical magnetotail parameters, we present Figs. 2 and 3. Figure 2 is a spectrum of unstable waves for $V_{di}/v_i = 1.0$ ($L_n/r_{Li} = 0.5$), $T_e/T_i = 0.5$, $m_e/m_i = 1/1836$, $\beta = 1.0$ and $\omega_{pe}^2/\Omega_e^2 = 125$. The growth rate has a relatively broad spectrum ($.5 < kr_{Le} < 5$) and achieves a maximum value of $\gamma_M \approx .21\,\omega_{\ell h}$ for $kr_{Le} \approx 1.2$. The real frequency exhibits the same qualitative behavior as the growth rate with a maximum value $\omega_M \approx .86\,\omega_{\ell h}$. Figure 3 plots the normalized maximum growth rate (as a function of k) versus V_{di}/v_i for $\beta = 0.25$, 1.00, 2.50 and $T_e/T_i = 0.5$, $\omega_{pe}^2/\Omega_e^2 = 125$ and $m_i/m_e = 1836$. We note that in the strong drift regime ($V_{di} > v_i$) that the growth rate can attain large values ($\gamma \sim \omega_{\ell h}$). Moreover, the stabilizing nature of β is clearly shown, a point which is

relevant to the magnetotail as will be seen in Section IV.

We comment that for $\underset{\sim}{k}\cdot\underset{\sim}{B} \neq 0$, the growth rate of the mode decreases due to electron Landau damping. The range of $k_{||}$ permitted can be determined from $\omega/k_{||} \geq 2v_e$ which can be written as

$$\frac{k_{||}}{k_\perp} \leq \frac{1}{4}\frac{V_{di}}{v_i}\left(\frac{T_i}{T_e}\right)^{\frac{1}{2}}\left(\frac{m_e}{m_i}\right)^{\frac{1}{2}}$$

where we have assumed $V_{di} < v_i$. Thus, the range of unstable waves in $k_{||}$ space is generally quite small.

We finally note that our model only considers $\underset{\sim}{B} = B_o\hat{e}_z$ which is reasonable since we are interested in localized spatial structures within the plasma sheet. However, it should be noted that the inclusion of a weak normal component does not alter our results. On the other hand, if the normal component of $\underset{\sim}{B}$ produces a radius of magnetic curvature comparable to the scale length of the ion pressure gradient, then the mode can be stabilized or destabilized depending on local plasma conditions (Krall and McBride, 1976).

C. Nonlinear Theory

Although the linear theory of the lower-hybrid-drift instability is well understood, this is not the case for the nonlinear theory of the instability. We briefly discuss each of the nonlinear analyses presented thus far, with an emphasis on obtaining estimates of the saturation amplitude of the unstable waves. This is perhaps the most important aspect of any nonlinear calculation since the functional form of the anomalous transport coefficients can be obtained from quasilinear theory, which treats the fluctuation amplitude approximately as a free parameter. Thus, a knowledge of the saturation energy (and its parametric dependence) obtained from a

nonlinear theory can be used to determine the associated anomalous transport properties of the instability in a straightforward manner based upon quasi-linear theory.

1. Quasilinear theory

Davidson (1977) has developed a quasilinear theory of the lower-hybrid-drift instability which is valid for electrostatic perturbations in the low drift velocity ($V_{di} < v_i$) and cold electron ($T_e \ll T_i$) regime. We comment that these results are insensitive to finite β electromagnetic corrections and can be applied to the magnetotail. He finds that stabilization can occur through either plateau formation in the ion distribution or current relaxation, depending upon the initial conditions of the plasma. These stabilization mechanisms are concerned with the kinetic form of the instability which is driven through an ion-wave resonance (i.e., $\gamma \propto \partial F_i/\partial v$). It is clear that if $\partial F_i/\partial v \to 0$ then $\gamma \to 0$ which corresponds to the formation of a plateau in the ion distribution. On the other hand, if the free energy available in the system (i.e., $W = \frac{1}{2} n m_e V_{di}^2 (1 + \frac{T_e}{T_i})^2$, the free energy available from the density inhomogeneity) is expended before $\partial F_i/\partial v = 0$, then the instability is stabilized by current relaxation and the saturation energy can be found by equating the <u>wave</u> energy density to the <u>free</u> energy density. We point out that this stabilization process is not appropriate if the system is being driven by an external force so that $W \approx$ constant. Following Davidson et al. (1977) it can be shown for a hydrogen plasma that (a) if $|V_{di}|/v_i > .18/(1 + T_e/T_i)$, then stabilization is due to current relaxation and the saturation energy is

$$\left(\frac{\epsilon_F}{nT_i}\right)^{cr}_{sat} = \frac{1}{4}\frac{m_e}{m_i}\frac{V_{di}^2}{v_i^2}\left(1+\frac{T_e}{T_i}\right)^2\left(1+\frac{\omega_{pe}^2}{\Omega_e^2}\right)^{-1} \qquad (17)$$

where $\epsilon_F = |\delta E_y|^2/8\pi$ is the field energy density of the electrostatic oscillations and the superscript cr denotes current relaxation, or

(b) if $|V_{di}|/v_i < .18/(1+T_e/T_i)$, then stabilization is due to plateau formation and the saturation energy is

$$\left(\frac{\epsilon_F}{nT_i}\right)^{pf}_{sat} = \frac{2}{45\sqrt{\pi}}\left(\frac{|V_{di}|}{v_i}\left(1+\frac{T_e}{T_i}\right)\right)^5\left(1+\frac{\omega_{pe}^2}{\Omega_e^2}\right)^{-1} \qquad (18)$$

where pf denotes plateau formation.

2. Ion trapping

Computer simulations of the lower-hybrid-drift instability by Winske and Liewer (1977) indicate that ion trapping stabilizes the instability in the strong drift velocity regime ($V_{di} \gtrsim 3\, v_i$). The instability is fluid-like in this regime and it is possible that a quasi-monochromatic wave develops so that ions can be trapped in its potential well. Winske and Liewer (1977) consider $\omega_{pe}^2/\Omega_e^2 \approx 1$ so that their results are not strictly applicable to the magnetotail plasma. However, one can obtain the following empirical expression for the saturation energy based on their results

$$\left(\frac{\epsilon_F}{nT_i}\right)^{it}_{sat} = 1.77 \times 10^{-2}\, k^2\lambda_{di}^2\left(1+\frac{2\omega_r^2}{k^2v_i^2}\right)^2 \qquad (19)$$

where $\lambda_{di} = v_i/\sqrt{2}\omega_{pi}$ is the ion Debye wavelength and the superscript "it" denotes ion trapping. Thus, ion trapping is expected to be an important stabilizing mechanism only in regions of very strong gradients (e.g., $L_n/r_{Li} \lesssim 1/6$.)

3. Electron resonance broadening

Huba and Papadopoulos (1978) have shown that electron resonance broadening can effectively stabilize the lower-hybrid-drift instability in finite β plasmas. This saturation mechanism can be understood as follows. From Eq. (8) it is clear that an electron-wave resonance can occur when

$$\frac{V_r^2}{v_e^2} = \frac{\omega}{k\bar{V}_B} \approx \frac{V_{di}}{\bar{V}_B} \approx \frac{1}{\beta}\frac{T_i}{T_e} \tag{20}$$

where V_r is the perpendicular electron resonant velocity. In the limit $\beta \to 0$ or $T_e \to 0$ it is seen that $V_r^2 >> v_e^2$ and hence, few electrons can participate in the resonance. On the other hand, when $\beta \approx 1$ and $T_e \approx T_i$ we find that $V_r^2 \approx v_e^2$ which permits a substantial number of electrons to be involved in the resonance. In fact, in this regime the electron-wave resonance can stabilize the instability (Davidson et al., 1977). Thus, in an initially unstable situation, it is possible that the ensuing turbulence may sufficiently broaden the electron-wave resonance to stabilize the instability (Dupree, 1967; Weinstock, 1969). However, numerical techniques are required to determine the saturation energy in the interesting regime $\beta \approx 1$ and $T_e \approx T_i$. We note that this saturation mechanism can produce steady state turbulence in contrast to the other stabilization processes discussed which only produce transient effects (Papadopoulos, 1977).

It is reasonable to expect $T_e \leq T_i$, $V_{di} \leq 3v_i$ and $\beta \sim O(1)$ for average plasma conditions in the magnetotail. For this parameter regime we anticipate that the dominant saturation mechanisms will be either current relaxation or electron resonance broadening. We present Fig. 4 which is a comparison of the saturation energies due to these stabilization processes as a func-

tion of T_e/T_i and V_{di}/v_i. We choose $\beta = 1$ and $\omega_{pe}^2/\Omega_e^2 = 100$. Clearly, current relaxation and electron resonance broadening are competitive processes in the regime $T_e \leqslant T_i$ and $V_{di} \leqslant v_i$. For inhomogeneities whose scale lengths are of the order of the mean ion Larmor radius or larger ($|V_{di}| \leqslant v_i$) we estimate the saturation energy to be $(\epsilon_F/nT_i)_{sat} \leqslant 10^{-5}$. We comment that the resonance broadening results include finite β electromagnetic corrections which is an extension of the work of Huba and Papadopoulos (1978).

III. Observational Results

In this section we briefly review the experimental evidence of electrostatic and magnetic noise observed by Gurnett et al. (1976) in the distant magnetotail. An excellent example of this turbulence is shown in Fig. 5 . These measurements were made by the IMP 8 spacecraft during a transit of the neutral sheet on April 18, 1974 and are typical of neutral sheet crossings.

The electrostatic noise occurs over a broad frequency range extending from about 10 Hz to a few kHz as may be seen in Fig. 5 . The frequency spectrum of the average electric field fluctuations during a high intensity burst (occurring during the time 1056 to 1059 UT on day 108) is shown in Fig. 6 . During this three minute period the local electron gyrofrequency was approximately 300 Hz, indicating that the largest field fluctuations occur for frequencies below the electron cyclotron frequency. Although instrumental limitations prevent measurement of very low frequencies, the spectral curve appears to be approaching a maximum in the vicinity of $f \approx 10$ Hz. Frequency-time spectograms indicate that the most intense noise is typically in the frequency range 10-70 Hz (see Fig. 7), indicating that the detailed three minute spectrum in Fig. 6 is not unusual. The frequency spectrum of the peak electrostatic fluctuations has the same shape as the average electrostatic fluctuations but with an amplitude 3-5 times the corresponding average fluctuation amplitude. The amplitude of the peak electrostatic fluctuations is in the range $|\delta E| = .05\text{-}5$ mV/m. Finally, we mention that the orientation of the

turbulent electric fields is observed to be within $\pm 20^{\circ}$ from the perpendicular to the ambient magnetic field.

The magnetic noise is observed in the frequency range $f \approx 10 - 600$ Hz and is strongly correlated with the electrostatic noise (as seen in Fig. 5) but occurs less frequently. The frequency spectrum of the magnetic fluctuations during the aforementioned intense electrostatic burst is shown in Fig. 8. This spectrum is similar to the electric field spectrum although the magnetic noise seems to be more bursty (since its peak to average ratio is large) which is consistent with its less frequent observation. The amplitude of this peak magnetic noise is in the range $|\delta B| = 1\text{-}100$ mγ. Unfortunately, the polarization of the magnetic field fluctuations could not be determined experimentally.

This microscopic turbulence is generally observed when the ambient magnetic field and plasma are turbulent, and when there are strong plasma flows ($V_F \approx 500\text{-}2000$ km/sec) toward or away from the Earth (Frank et al., 1976). A typical turbulent state is illustrated in Fig. 9 which plots the magnitude of the ambient magnetic field, proton density, proton temperature and proton bulk velocity for 1030-1100 UT on day 108. The magnetic field is measured on a 1.28 sec average and the plasma data on an 82 sec average. The flow velocity and proton temperature have not been plotted for 1046-1056 since the proton density is very low and the LEPEDEA measurements are not entirely reliable. We mention that a detailed analysis of a "fireball" event by Coroniti et al. (1977) demonstrated that the magnetic field can be turbulent on time scales ≤ 1 sec, indicating the possibility of sharp gradients ($L \approx r_{Li}$) which will be considered in the next section.

It is clear that even in as short a period as 30 minutes the satellite moved through a variety of plasma conditions. The magnetic field ranged from a few γ up to 35 γ, the density from .01 cm^{-3} to 1.6 cm^{-3}, the proton temperature from 1 kev to 10 kev and the flow velocity from 300 km/sec to 1600 km/sec. Based on this data we find that β, an important parameter in determining the existence and behavior of the lower-hybrid-drift instability, varies from 10^{2} to 10^{-2} over this period. This point is further discussed in the following section.

IV. Comparison of Theory and Observational Results

In this section we compare the theoretical predictions of microturbulence associated with the lower-hybrid-drift instability discussed in Section II with the recent satellite observations of electric and magnetic field fluctuations in the magnetotail (Gurnett et al, 1976) detailed in Section III.

In particular, we demonstrate that the agreement of theory and experiment on such points as existence conditions for the instability, polarization of the turbulence, nature of the frequency spectrum of the fluctuations and amplitude of the fluctuations is remarkably good. The detailed agreement of theory and experiment argues convincingly that the lower-hybrid-drift instability has been directly observed in the magnetotail. This is important, not only because this instability may be important in regulating magnetotail dynamics (e.g., reconnection and the triggering of magnetic substorms) but it represents the first direct observation of an instability which is considered to be very important in several high β laboratory plasma devices (e.g., theta pinches, reversed field pinches).

The most striking feature of the satellite observations of Gurnett, et al. (1976) is the strong correlation between the occurrence of electrostatic and electromagnetic noise, and the presence of fluctuating magnetic fields (see Fig. 5 and the discussion in Section III). The fluctuating magnetic fields imply the presence of magnetic field gradients and furthermore, in situations where the plasma beta is of order unity, gradients in the plasma density and temperature. Even in situations where the magnetic field is relatively strong and constant, there may exist density and temperature gradients if $\beta \ll 1$. In the theory of the lower-hybrid-drift

instability discussed in Section II, we saw that plasma gradients with scale-length satisfying

$$\frac{L_n}{r_{Li}} < \left(\frac{m_i}{m_e}\right)^{\frac{1}{4}}$$

were required to excite the lower-hybrid-drift instability. For typical tail parameters ($T_i \sim 2$kev and $B \sim 15\gamma$) it is found that $r_{Li} \sim 300$ km so that the instability can be excited for $L_n \leq 2.0 \times 10^3$ km. However, as noted earlier, for gradient scale lengths such that $(m_i/m_e)^{\frac{1}{2}} < L_n/r_{Li} < (m_i/m_e)^{\frac{1}{4}}$, the mode transforms into the drift cyclotron instability (Freidberg and Gerwin, 1977; Gladd and Huba, 1978) which has a characteristic frequency and growth rate $\omega_r \sim \ell\Omega_i$ and $\gamma \sim \ell\,(m_e/m_i)^{\frac{1}{4}}\,\Omega$, respectively. Thus, instability can persist even for $L_n \sim 1.2 \times 10^4$ km.

Although the existence of gradients is obvious in Fig. 9, it is somewhat difficult to ascertain their magnitude because the satellite offers only one reference point from which to observe magnetic field and plasma quantities, which can vary both in space and time. Indeed, the observations of plasma flow by the satellite shows flow velocities ranging up to 1600 km/sec and are much larger than the average satellite velocity in the distant magnetotail (≈ 2 km/sec). We can estimate the gradient length scale from $L = |\underset{\sim}{V}_F + \underset{\sim}{V}_s|\,\Delta t \approx V_F \Delta t$ where Δt is the time over which the magnetic field or density changes appreciably, $\underset{\sim}{V}_F$ is the flow velocity of the plasma and $\underset{\sim}{V}_s$ is the velocity of the satellite. If we consider Fig. 9, we find that the gradient length scale in a turbulent region is $L \approx 60{,}000$ km where $V_F \approx 1000$ km/sec and $\Delta t \approx 60$ sec. Since we have assumed the ion Larmor radius is $r_{Li} \approx 50$-400 km, we find that $L/r_{Li} \approx 150$-1200

which is too weak to excite the lower-hybrid-drift instability. However, the profiles in Fig. 9 do not rule out the presence of sharper gradients as mentioned in Section III. The microscopic structure of the magnetic field in a turbulent part of the magnetotail has been studied in detail by Coroniti et al. (1977). In particular, Fig. 3 of this reference indicates that magnetic field gradient scale lengths can be as strong as $L \sim r_{Li}$. Unfortunately, measurements of density and temperature can only be made on an 82 sec average and the direct observation of sharp plasma gradients is not possible. However, if we consider the plasma to be in equilibrium locally, then we expect $L_n \propto L_B \beta$ where L_B is the scale length of the magnetic field inhomogeneity, and we can infer the existence of sharp plasma density gradients. Therefore, we see that in the turbulent plasma sheet, there can be ample plasma and field gradients of sufficient sharpness to excite the lower-hybrid-drift instability.

Having shown that the existence conditions for the lower-hybrid-drift instability can be met in the magnetotail, we now use the theory of Section II to account for features of the electrostatic and electromagnetic noise First, we consider the polarization of the electrostatic noise. In developing the electrostatic theory it was found that the most rapidly growing part of the lower-hybrid-drift spectrum typically satisfies $\underline{k} \times \delta\underline{E} \approx 0$ and $\delta\underline{E} \cdot \underline{B}_o \approx 0$. In Gurnett et al. (1976) it is shown that during a thirty minute period in which the direction of the magnetic field was well established, the polarization of the electrostatic noise was always within $\pm 20^\circ$ of perpendicular to the magnetic field, thus consistent with the theoretical prediction that the most rapidly growing modes would be flute-like ($\underline{k} \cdot \underline{B} \approx 0$). Although the lower-hybrid-drift instability is

damped at large angles, propagation effects in an inhomogeneous medium may account for the observed angular distribution of the fluctuating electric field.

We next address the question of the relationship of the electrostatic and the electromagnetic noise. In the theory of the lower-hybrid-drift instability it is found that in a finite β plasma, the important field components are δE_y and δB_z with

$$\frac{|\delta B_z|}{|\delta E_y|} \cong \beta_i^{\frac{1}{2}} \left(\frac{\omega_{pe}}{\Omega_e} \right) 10^8 \text{ mV} \qquad (21)$$

where δE_y is measured in mV/meter. Equation (21) is obtained in the approximation $L_n/r_{Li} > 1$ and $T_e/T_i \ll 1$. Therefore, when the plasma β_i is finite, the satellite should observe fluctuations in both δE_y and δB_z. The fact that the electrostatic noise is observed more frequently than the electromagnetic noise may be due to the relative sensitivty of the measuring devices, (i.e., the magnetic field detectors are not as sensitive as the electric field detectors). We note that in Eq. (21), the relationship $|\delta B_z|/|\delta E_y|$ is independent of the driving mechamism (i.e., L_n/r_{Li}) and we should see large $|\delta B_z|$ whenever we see large $|\delta E_y|$. This is borne out by the experimental observations (Fig. 5) in which we see that observation of electromagnetic noise is almost always attendant to the occurrence of exceptionally strong bursts of electrostatic noise.

As another example of finite β effects on the lower-hybrid-drift instability we note that if $T_e \leq T_i$, finite β is a strong stabilizing effect on the instability (see Fig. 3). Close examination of the electrostatic turbulence that occurs during the thirty minute time period

illustrated in Fig. 9 shows that the noise level in the last half of that time period is as much as four orders of magnitude larger than the noise in the first half. Examination of the profiles in Fig. 9 indicate that the average plasma β during the latter half of the period is much lower than the average plasma β during the first half. This is strongly suggestive that the instability was finite β stabilized (or at least substantially curtailed) in growth during the first half, as would be expected from the theory.

Next, we turn our attention to the question of whether the frequency spectrum of the electrostatic noise is consistent with the theoretical predictions of the lower-hybrid-drift instability. First, consider the spectrum illustrated in Fig. 2. We note that the k spectrum is quite broad (γ substantial for $.5 < kr_{Le} < 5$) while the real frequency in this range varies only by a factor of two. Therefore, we might expect to see a relatively narrow frequency spectrum centered about $\omega_{\ell h}$. The actual center frequency will depend on the sharpness of the gradient exciting the mode. However, the frequency observed by the satellite includes the relevant Doppler shifts since, in general, proton bulk flows are not directed parallel to the local magnetic field vector (Frank et al., 1976). Thus,

$$f_{obs} = f + \frac{\underline{k}\cdot\underline{V}_s}{2\pi} + \frac{\underline{k}\cdot\underline{V}_F}{2\pi} \qquad (22)$$

Typically $V_F \gg V_s$ so that

$$f_{obs} \sim f \pm \frac{kV_F}{2\pi}\cos\phi \qquad (23)$$

For typical tail parameters we estimate the range of wavenumbers excited to be $k \approx .2\text{-}5\ \text{km}^{-1}$ with maximum growth occuring at $k_M \approx 1\ \text{km}^{-1}$. Moreover, if we let V_F = 500-1500 km/sec, $f \sim f_{\ell h} \sim 3\text{-}20$ Hz and $\cos\phi \sim \frac{1}{2}$ it is found that

$$f_{obs} \approx 10\text{-}600 \text{ Hz}$$

with the maximum instensity $\left(f_{obs}^{M}\right)$ in the range

$$f_{obs}^{M} \approx 20\text{-}60 \text{ Hz},$$

which is consistent with the observations of Gurnett et al. (1976) (see Fig. 7). Thus, while the theory of Section II predicts a relatively narrow frequency spectrum, the dominance of the Doppler shifting term $\underset{\sim}{k} \cdot \underset{\sim}{V}_F$ in Eq.(23)acts to substantially broaden the observed spectrum.

Furthermore, the Doppler shift explains the energy frequency spectra (Figs. 6 and 8) discussed in the previous section. In these figures the amplitude of fluctuations decreases with increasing frequency. From nonlinear considerations we find that as k increases above k_M, the saturation energy of the excited waves decreases. Moreover, since these waves are strongly Doppler shifted to higher frequencies, we expect that the energy density of the unstable waves to be a decreasing function of frequency for $\omega > \omega_M$, which is consistent with Figs. 6 and 8.

Finally, we consider whether the theoretical amplitudes of the electrostatic and electromagnetic noise are consistent with observations. In Section II, several saturation mechanisms which could stabilize the lower-hybrid-drift instability were discussed. It is

not clear which of these mechanisms is dominant or, as might reasonably be expected, there are mechanisms which might be important under some plasma conditions, and not under others. For purposes of comparison with observation, we determine the strengths of the fluctuating fields using the estimate of the saturation energy based upon current relaxation. The amplitude of the electric field fluctuations is

$$|\delta E| = (\pi n m_e V_{di}^2)^{\frac{1}{2}} (1+T_e/T_i)\ (1+\omega_{pe}^2/\Omega_e^2)^{-\frac{1}{2}}$$

and the amplitude of the magnetic fluctuations is

$$|\delta B| = \frac{v_i}{c} \left(\frac{m_i}{m_e} \right)^{\frac{1}{2}} \frac{\omega_{pe}^2}{\Omega_e^2} |\delta E| 10^8 \text{ m}\gamma .$$

For conditions typical of the magnetotail (e.g., T_i = 1 keV, B = 20 γ, n ~ .01-1 cm^{-3}, $T_e \ll T_i$ and $V_{di} \leq v_i$) we find from Eqs. (19) and (20) that $|\delta E|$ ~ .2-6 mV/m and $|\delta B|$ ~ .09-270 mγ which is consistent with experimental evidence, where the amplitude of the peak electric field fluctuations is observed to be in the range of $|\delta E|$ ~ .05-5 mV/m and that of the magnetic field fluctuations is $|\delta B|$ ~ 1-100 mγ.

V. Conclusions and Discussion

We have demonstrated that our theoretical prediction of plasma turbulence in the magnetotail due to the lower-hybrid-drift instability (Huba et al., 1977) is substantiated by experimental observations of electrostatic and magnetic turbulence in the distant magnetotail (Gurnett et al., 1976). In particular, we have shown that existence conditions for the lower-hybrid-drift instability can be met (i.e., there seem to exist sharp, localized gradients within a much broader plasma sheet). Secondly, we have shown that observations of the frequency spectrum and polarization are in good agreement with the predictions of our linear stability analysis. Thirdly, we have shown that the observed amplitude of fluctuations is consistent with the nonlinear analysis of the lower-hybrid-drift mode. Finally, we point out that both the electrostatic and the magnetic fluctuations observed by Gurnett et al. (1976) may be explained by this single instability. In addition to discussing the specific points above, we have presented a short review of the theory of the lower-hybrid-drift instability because of its relative newness to the space physics community. We now address several other topics pertinent to the problem of microturbulence in the magnetotail.

The theory of the lower-hybrid-drift instability discussed in this work has emphasized the physical nature of the instability and retained only the fundamental aspects of the plasma configuration (e.g., magnetic field and density inhomogeneities, finite β). However, in the turbulent plasma sheet other aspects of the plasma environment can be important at times which affect the lower-hybrid-drift instability, such as temperature gradients (Davidson et al., 1977; Krall and McBride, 1976), magnetic shear (Krall, 1977; Gladd et al., 1977; Davidson et al., 1978) and magnetic curvature (Krall and McBride, 1976). The inclusion of all these

effects is beyond the scope of this paper. We point out that although the instability theory presented here is incomplete, the instability is viable for a variety of plasma conditions typical of the magnetotail.

The most important aspect of the observed turbulence is that it strongly suggests anomalous transport is indeed a major factor in the evolution of macroscopic processes such as field line merging, tearing instabilities or "fireballs" (Frank et al., 1976; Coroniti et al.. 1977). Probably the only tractable method for realistically describing such macroscopic events is through the use of multi-fluid plasma codes which incorporate anomalous transport coefficients based upon the relevant microscopic physical phenomena. The evidence presented in this paper indicates we may proceed with some confidence to use the anomalous transport properties associated with the lower-hybrid-drift instability in a multi-fluid code to model macro-processes in the magnetotail. We are presently developing such a code for the purposes of understanding reconnection in the magnetotail.

We comment that a problem encountered when invoking the lower-hybrid-drift instability as a source of anomalous resistivity for magnetic field line reconnection is the absence of instability near magnetic nulls. This is because as $B \to 0$ one expects $\beta \to \infty$ and the instability is easily stabilized (e.g., see Fig. 2 of Huba et al., 1977). Moreover, near a magnetic null the electron orbits become complex and are no longer describable by the guiding center drift approximation used in the theory. However, a model of the magnetotail with a well defined neutral line embedded in the plasma sheet is a considerable over simplification of the physical situation. In fact, the plasma sheet is a very turbulent

medium as shown by Gurnett et al. (1976), Frank et al. (1976) and Coroniti et al. (1977). Thus, we suggest that the lower-hybrid-drift instability (and possibly other instabilities) produce small scale "clumps" of electrostatic turbulence throughout the magnetotail and that electrons can be effectively scattered by these "clumps". A macroscopic anomalous resistivity can then exist in the magnetotail based on a statistical description of these "clumps" and the absence of turbulence at a single magnetic null point is of little consequence.

Within the context of this concept of anomalous resistivity produced by small scale "clumps" of lower-hybrid-drift turbulence, we suggest a mode-mode coupling process may occur in the magnetotail; similar to that which occurs in the ionosphere. Ionospheric irregularities have been observed with scale lengths from a few meters to a few kilometers (Dyson et al., 1974). Since no single instability has been found which can explain the entire range of irregularities, the prevailing theories (Sudan et al., 1973; Chaturvedi and Kaw, 1976)

invoke a two-step process. A long wavelength instability (e.g., Rayleigh-Taylor instability) is excited which can nonlinearly produce short wavelength drift waves. We propose a similar phenomenon may exist in the magnetotail, whereby a macroscopic MHD instability (e.g., kink or tearing mode) can produce local gradients in density and magnetic field which can excite short wavelength modes such as the lower-hybrid-drift instability. The anomalous resistivity produced by the ensuing "clumps" of electrostatic turbulence will in turn affect the evolution of the large scale disturbance. We are presently investigating this possibility

and hope to eventually perform a numerical simulation which will self-consistently follow this process.

Finally, we reiterate that the lower-hybrid-drift instability is an important anomalous transport mechanism in many laboratory plasma confinement devices such as theta pinches, reversed field pinches and mirror machines. Coincidentally, many of the important dimensionless quantities which determine the behavior of this instability are the same for both the laboratory and magnetotail plasmas (e.g., $\omega_{pe}^2 \gg \Omega_e^2$, $\beta \sim 1$, $V_{di} \sim v_i$), even though the density and magnetic field differ by many orders of magnitude. Unfortunately, the lower-hybrid-drift instability cannot be observed directly in laboratory experiments since its time scale is extremely short ($t_{\ell h} = f_{\ell h}^{-1} \sim 10^{-9}$ sec). Thus, the magnetotail may be the ideal laboratory to study the lower-hybrid-drift instability because in situ measurements can be made. The information obtained from such studies may prove to be very valuable to the ongoing research in plasma confinement experiments and fusion research.

Acknowledgements

We gratefully acknowledge Don Gurnett for calling our attention to the observational measurements and for several valuable discussions. We also wish to thank Don Gurnett and Kent Ackerson for providing field fluctuation and particle data, respectively, and Ron Lepping for providing magnetometer data. Finally, we thank Geary Voots and Mark Baumbach for their assistance in preparing the fluctuation data.

This research has been supported by ONR and NASA.

References

Ashour-Abdalla, M., and C. F. Kennel, Convective Cold Upper Hybrid Instabilities, in Magnetospheric Particles and Fields, edited by B. M. McCormac, D. Reidel, Dordrecht, Netherlands, in press, pp. 181-196, 1976.

Commisso, R. J. and H. R. Griem, Observation of Collisionless Heating and Thermalization of Ions in a Theta Pinch, Phys. Rev. Lett., 36, 1038, 1976.

Chaturvedi, P. K. and P. Kaw, An Interpretation for the Power Spectrum of Spread F Irregularities, J. Geophys. Res., 81, 3257, 1976.

Coroniti, F. V., F. L. Scarf, L. A. Frank and R. P. Lepping, Microstructure of a Magnetotail Fireball, Geophys. Res. Lett., 4, 219, 1977.

Davidson, R. C. and N. T. Gladd, Anomalous Transport Properties Associated with the Lower-Hybrid-Drift Instability, Phys. Fl., 18, 1327, 1975.

Davidson, R. C., N. T. Gladd, C. S. Wu and J. D. Huba, Influence of Finite-β Effects on the Lower-Hybrid-Drift Instability in Post-Implosion θ Pinches, Phys. Rev. Lett., 37, 750, 1976.

Davidson, R. C., N. T. Gladd, C. S. Wu and J. D. Huba, Effects of Finite Plasma Beta on the Lower-Hybrid-Drift Instability, Phys. Fl., 20, 301, 1977.

Davidson, R. C., Quasilinear Stabilization of the Lower-Hybrid-Drift Instability in Post-Implosion Theta Pinches, (submitted for publication to Phys. Fl., 1977).

Davidson, R. C. and N. T. Gladd, "Influence of Strong Inhomogeneities in High-Frequency Mirror-Drift-Cone and Convective-Loss-Cone Instabilities," Phys. Fl., 20, 1516, 1977.

Davidson, R. C., N. T. Gladd and Y. Goren, Influence of Magnetic Shear on the Lower-Hybrid-Drift Instability - With Application to Microstability Properties of Toroidal Reversed-Field Pinches, (submitted for publication to Phys. Fl., 1978).

Dyson, P. L., J. P. McClure and W. B. Hanion, In Situ Measurements of the Spectral Characteristics on Ionospheric Irregularities,

Dupree, T. H., Nonlinear Theory of Drift-Wave Turbulence and Enhanced Diffusion, Phys. Fl., 10, 1049, 1967.

Frank, L. A., K. L. Ackerson, and R. P. Lepping, On Hot Tenuous Plasmas, Fireballs, and Boundary Layers in the Earth's Magnetotail, J. Geophys. Res., 81, 5859, 1976.

Fredricks, R. W., Plasma Instability at $(n+\frac{1}{2})f_c$ and its Relationship to Some Satellite Observations, J. Geophys. Res., 76, 5344, 1971.

Freidberg, J. P. and R. A. Gerwin, Lower-Hybrid-Drift Instability at Low Drift Velocities, Phys. Fl., 20, 1311, 1977.

Gladd, N. T., The Lower-Hybrid-Drift Instability and the Modified Two-Stream Instability in High Density Theta Pinch Environments, Plasma Phys., 18, 27, 1976.

Gladd, N. T., Y. Goren, C. S. Liu and R. C. Davidson, Influence of Strong Inhomogeneities and Magnetic Shear on Microstability Properties of the Tormac Sheath, Phys. Fl., 20, 1876, 1977.

Gladd, N. T. and J. D. Huba, Finite Beta Effects on the Drift Cyclotron Instability, submitted to Phys. Fl., 1978.

Gurnett, D. A., L. A. Frank, and R. P. Lepping, Plasma Waves in the Distant Magnetotail, J. Geophys. Res. , 81, 6059, 1976.

Hoh, F. C., Stability of Sheet Pinch, Phys. Fl., 9, 277, 1966.

Huba, J. D. and C. S. Wu, Effects of a Magnetic Field Gradient on the Lower-Hybrid-Drift Instability, Phys. Fl., 19, 988, 1976.

Huba, J. D., N. T. Gladd and K. Papadopoulos, The Lower-Hybrid-Drift Instability as a Source of Anomalous Resistivity for Magnetic Field Line Reconnection, Geophys. Res. Lett., 4, 125, 1977.

Huba, J. D. and K. Papadopoulos, Nonlinear Stabilization of the Lower-Hybrid Drift Instability by Electron Resonance Broadening, Phys. Fl., 21 121, 1978.

Krall, N. A. and P. C. Liewer, Low Frequency Instabilities in Magnetic Pulses, Phys. Rev., A4, 2094, 1971.

Krall, N. A. and J. B. McBride, Magnetic Curvature and Ion Distribution Function Effects on Lower-Hybrid-Drift Instabilities, Phys. Fl., 19, 1970, 1976.

Krall, N. A., Shear Stabilization of Lower Hybrid Drift Instabilities, Phys. Fl., 20, 311, 1977.

Lemons, D. S. and S. P. Gary, Electromagnetic Effects on the Modified Two Stream Instability, J. Geophys. Res., 82, 2337, 1977.

McBride, J. B., E. Ott, J. P. Boris and J. H. Orens, Theory and Simulation of Turbulent Heating by the Modified Two-Stream Instability, Phys. Fl. 15, 2367, 1972.

Mikhailovskii, A. B. and Timofeev, A. V., "Theory of Cyclotron Instability in a Non-Uniform Plasma," Sov. Phys. JETP, 17, 626, 1963.

Papadopoulos, K., A Review of Anomalous Resistivity for the Ionosphere, Rev. Geophys. and Space Phys., 15, 113, 1977.

Sudan, R. N., J. Akinrimisi and D. T. Farley, Generation of Small-Scale Irregularities in the Equatorial Electrojet, J. Geophys. Res., 78, 240, 1973.

Weinstock, J., Formulation of a Statistical Theory of Strong Plasma Turbulence, Phys. Fl., 12, 1045, 1969.

Winske, D. and P. C. Liewer, Particle Simulation Studies of the Lower-Hybrid-Drift Instability, (submitted for publication to Phys. Fl., 1977).

Young, T. S., J. D. Callen, and J. E. McCune, High-Frequency Electrostatic Waves in the Magnetosphere, J. Geophys. Res., 78, 1082, 1973.

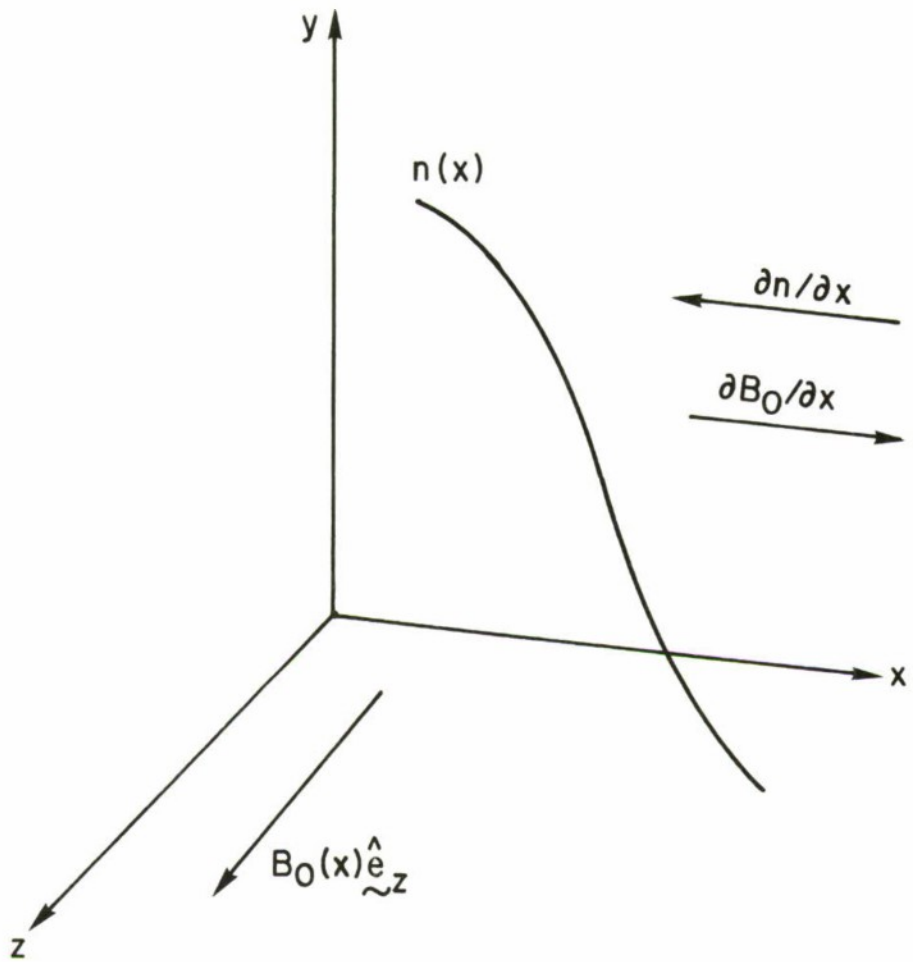

Fig. 1 — Slab geometry and background plasma configuration

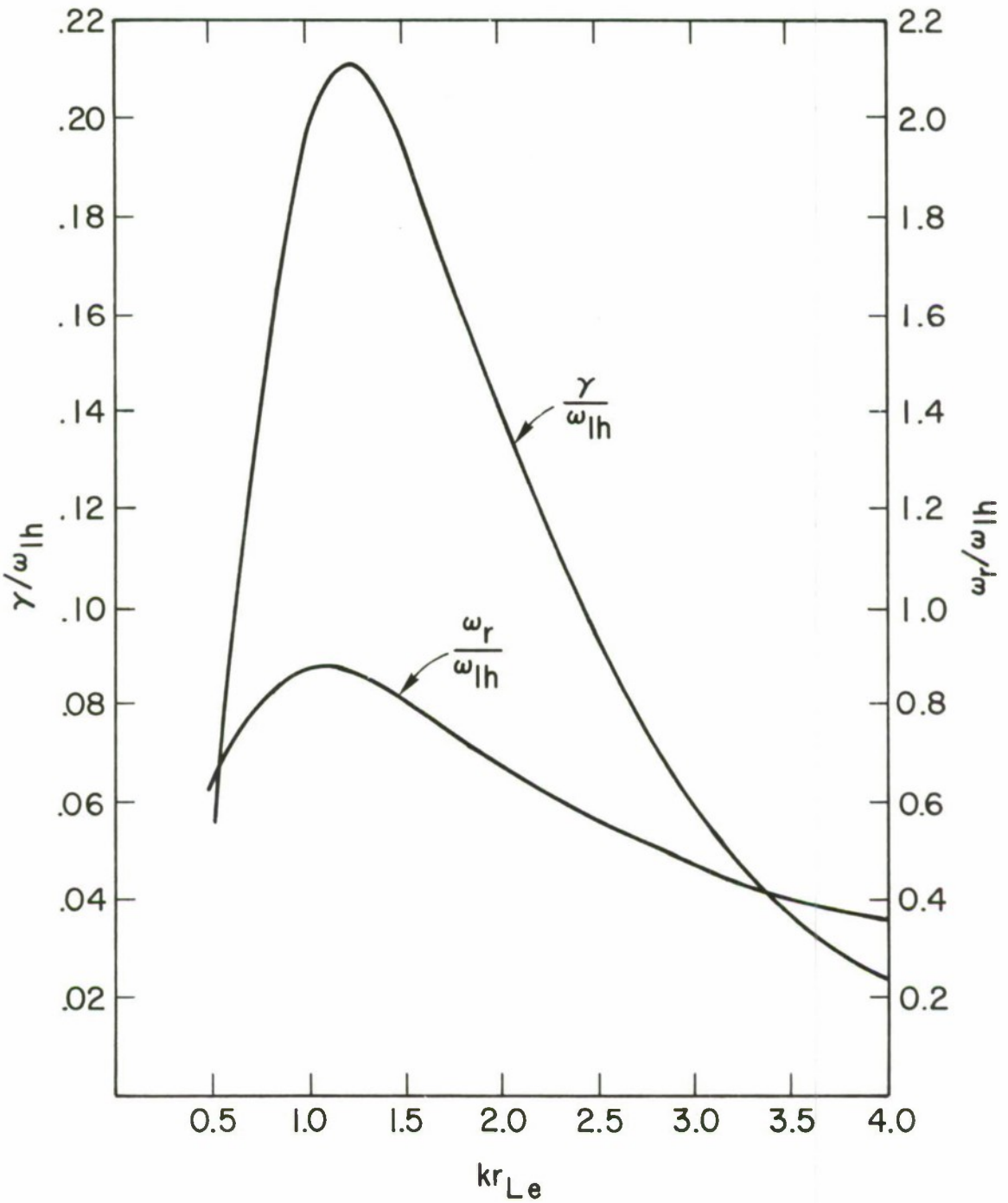

Fig. 2 — Spectrum of unstable lower-hybrid-drift waves for $V_{di}/v_i = 1.0$, $T_e/T_i = 0.5$, $m_e/m_i = 1/1836$, $\beta = 1.0$ and $\omega_{pe}^2/\Omega_e^2 = 125$

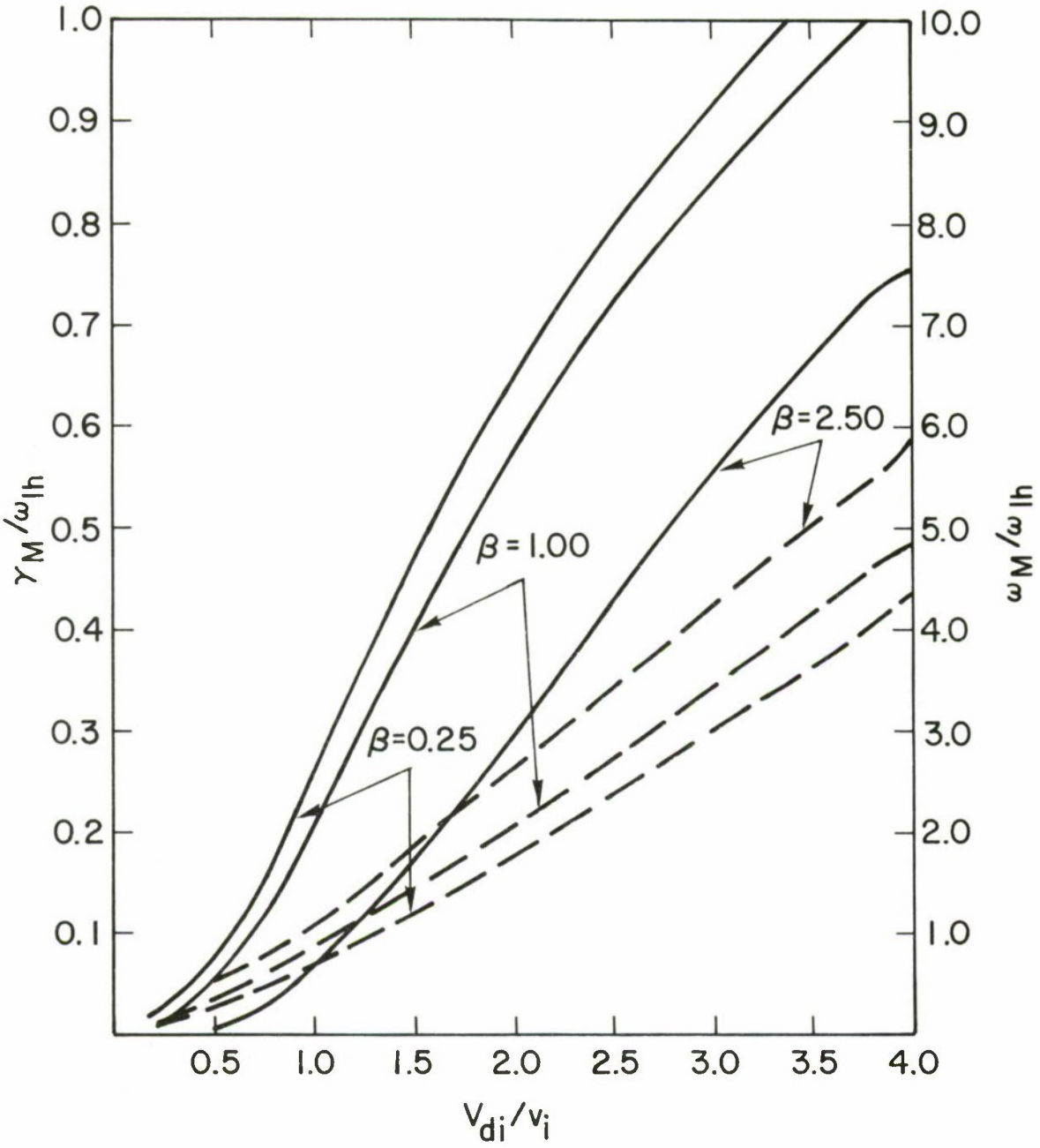

Fig. 3 — Maximum growth rate (solid line) and corresponding real frequency (dashed line) versus V_{di}/v_i for β = 0.25, 1.00, 2.50, and T_e/T_i = 0.5, m_e/m_i = 1/1836 and ω_{pe}^2/Ω_e^2 = 125

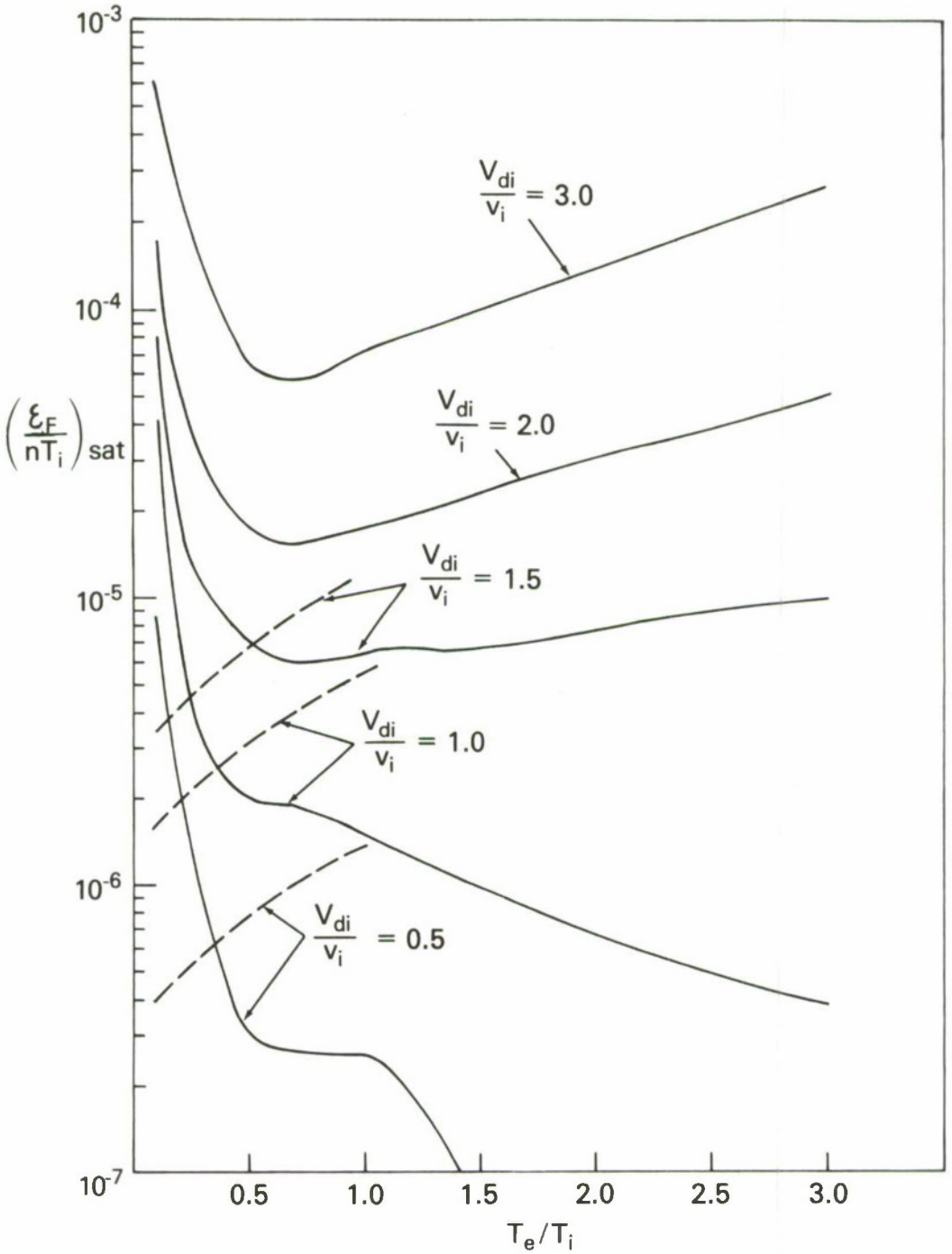

Fig. 4 — Saturation energy due to electron resonance broadening (solid line) and current relaxation (dashed line) as a function of T_e/T_i and V_{di}/v_i for $\beta = 1.0$ and $\omega_{pe}^2/\Omega_e^2 = 100$

Fig. 5 — Magnetic field and plasma wave measurements made by the Imp 8 spacecraft for day 108 during a transit of the neutral sheet (Gurnett et al., 1971). Note the intense electrostatic and magnetic noise bursts which occurred throughout the day.

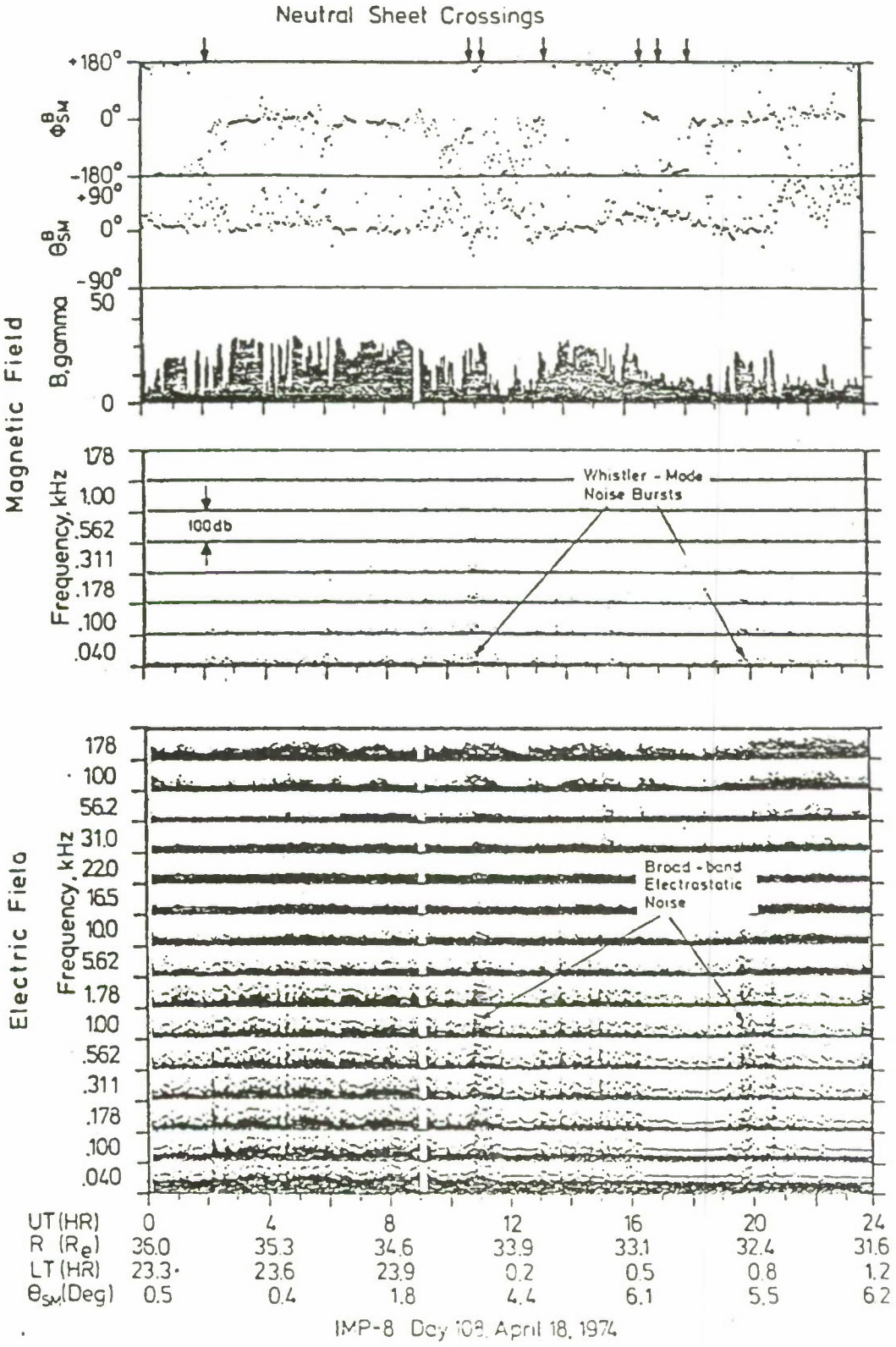
Neutral Sheet Crossings
Magnetic Field
+180°
0°
-180°
Φ^B_{SM}
+90°
0°
-90°
θ^B_{SM}
50
0
B,gamma
178
1.00
.562
.311
.178
.100
.040
Frequency, kHz
100db
Whistler - Mode
Noise Bursts
Electric Field
178
100
56.2
31.0
22.0
16.5
10.0
5.62
1.78
1.00
.562
.311
.178
.100
.040
Frequency, kHz
Broad - band
Electrostatic
Noise
UT(HR) 0 4 8 12 16 20 24
R (R_e) 36.0 35.3 34.6 33.9 33.1 32.4 31.6
LT(HR) 23.3 23.6 23.9 0.2 0.5 0.8 1.2
θ_{SM}(Deg) 0.5 0.4 1.8 4.4 6.1 5.5 6.2
IMP-8 Day 108, April 18, 1974

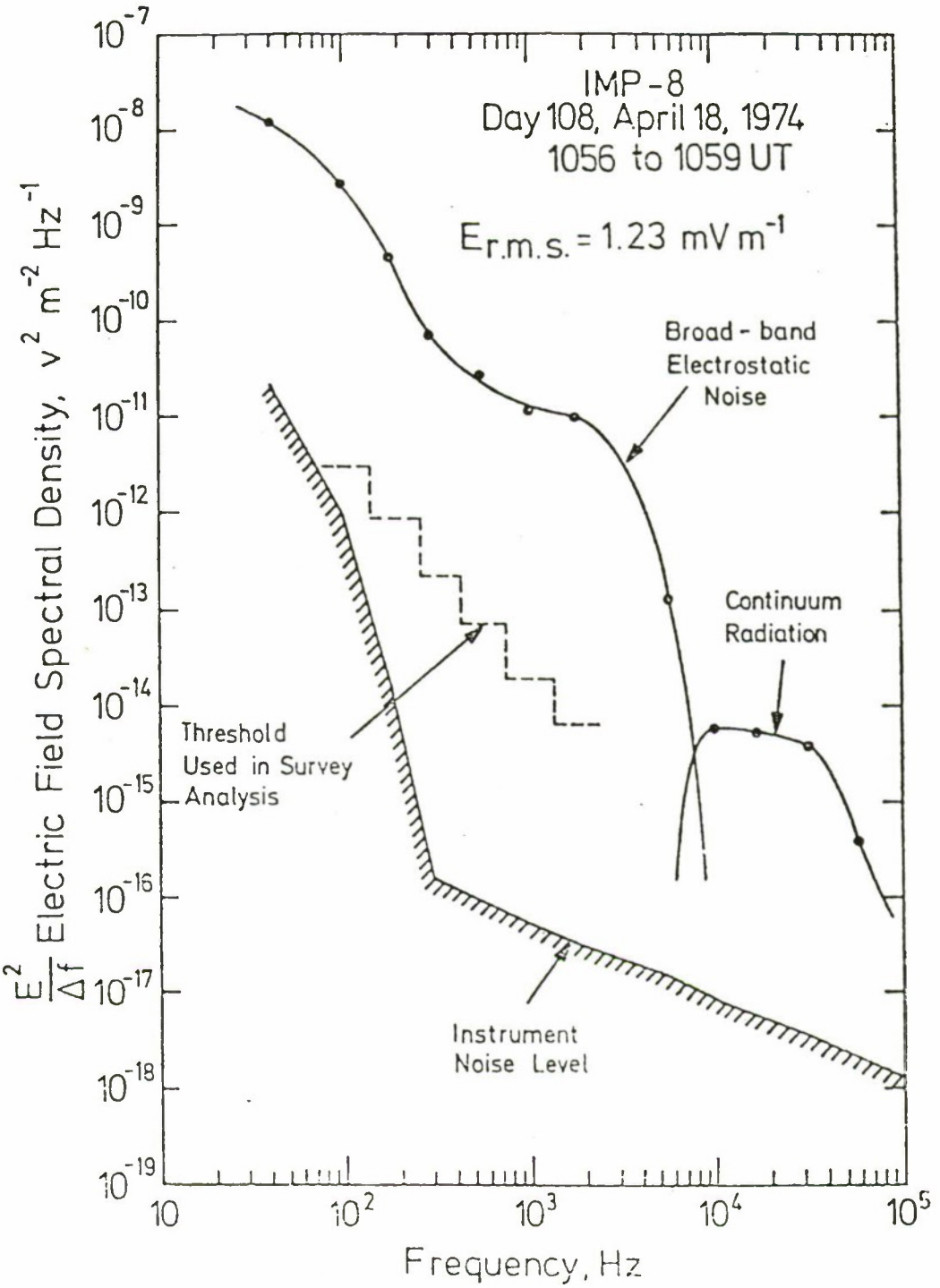

Fig. 6 — A typical spectrum of broadband electrostatic noise during a period of relatively high intensity, from 1056 to 1059 UT on day 108 (Gurnett et al., 1971)

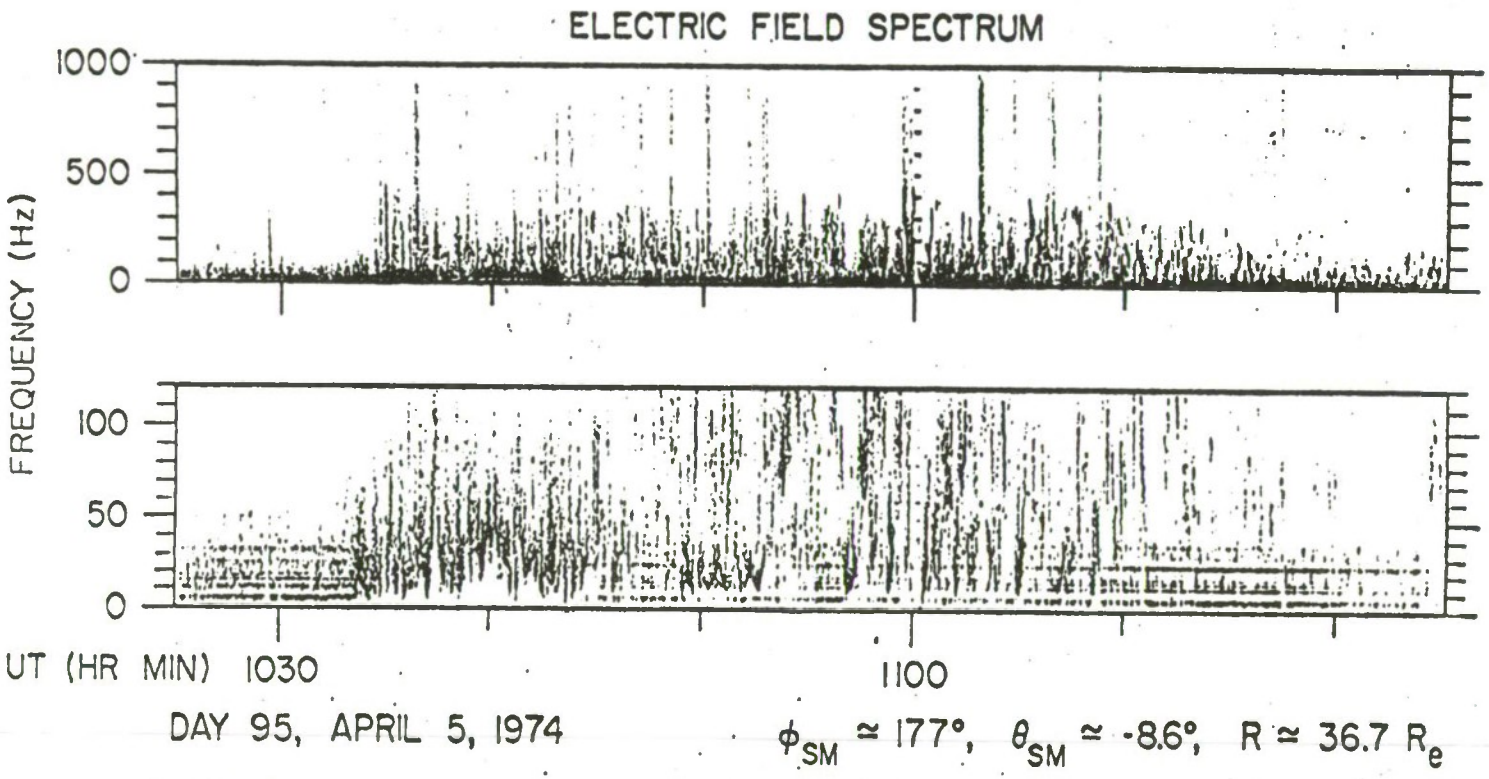

Fig. 7 — Frequency-time spectrogram of the broad band electrostatic noise. Note that the most intense noise is in the range 10-70 Hz. (Gurnett et al., 1976).

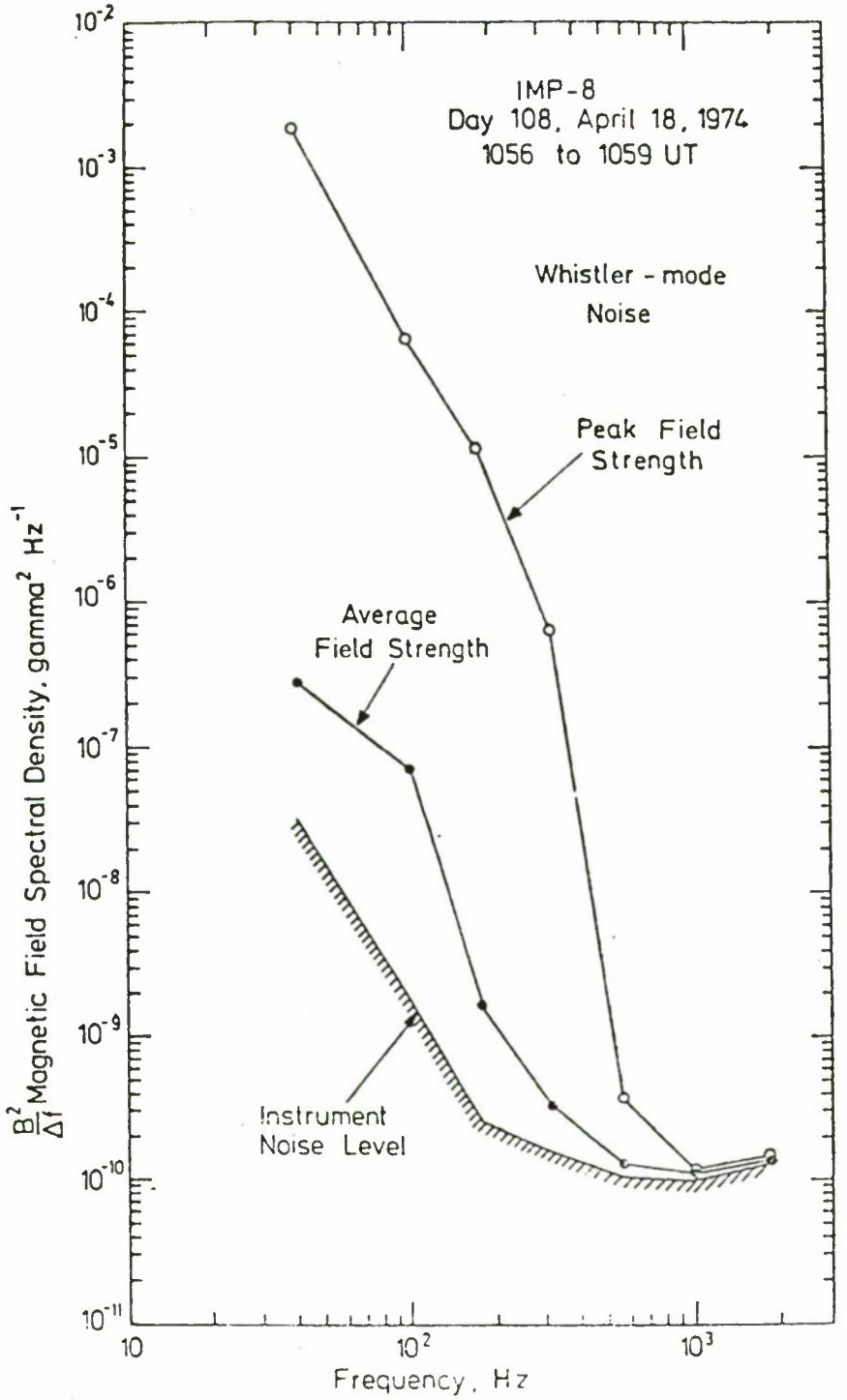

Fig. 8 — Typical spectrum of magnetic noise from 1056 to 1059 UT on day 108 (Gurnett et al., 1976)

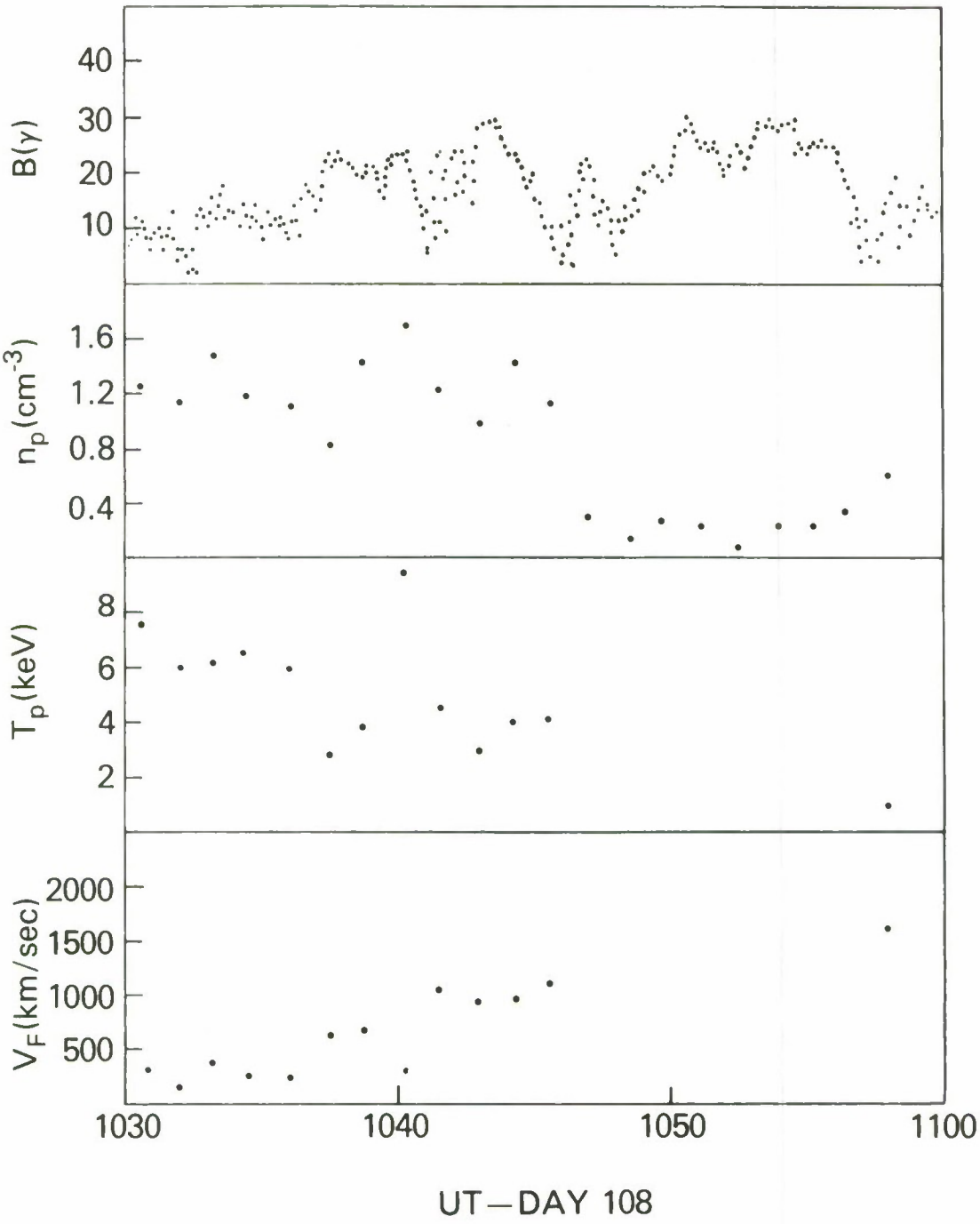

Fig. 9 — Ambient magnetic field strength (Lepping, private communication), proton density, proton temperature and proton bulk velocity (Ackerson, private communication) for 1030 to 1100 UT on day 108. Note that the magnetic field was very turbulent during this period. The data points for the bulk flow velocity and proton temperature are not shown for 1046-1056 UT since the proton density is very low and the LEPEDEA measurements are not entirely reliable.

DISTRIBUTION LIST

University of Alaska
Geophysical Institute
Fairbanks, Alaska 99701
Attn: S. I. Akasofu
Attn: J. R. Kan
Attn: Library

University of Arizona
Dept. of Planetary Sciences
Tucson, Arizona 85721
Attn: J. R. Jokipii

Boston College
Chestnut Hill, Mass. 02167
Attn: R. L. Carovillano

Boston University
Dept. of Astrophysics
Boston, Massachusetts 02215
Attn: M. Papagianis

University of California, S. D.
LaJolla, California 92037
Physics Dept.- Attn: J. A. Fejer
Attn: T. O'Neil
Attn: Library
Dept. of Applied Sciences - Attn: H. Booker

University of California
Los Angeles, California 90024
Physics Dept. - Attn: J. M. Dawson
Attn: B. Fried
Attn: J. G. Moralles
Attn: A. Wong
Attn: Library
Inst. of Geophysics & Planetary Physics - Attn: Library
Attn: C. Kennel
Attn: C. Russel
Attn: F. Coroniti
Attn: M. Kivelson
Attn: R. Thorme
Attn: R. McPherron
Dept. of Eng. & Applied Sciences - Attn: R. J. Armstrong

University of California
Berkeley, California 94720
Space Sciences Laboratory - Attn: Library
Attn: F. Mozer
Attn: R. P. Lin
Attn: M. Hudson
Attn: K. Anderson

University of California
Berkeley, California 94720
Phys. Dept. - Attn: Library
Attn: C. McKee

University of California
Physics Dept.
Irvine, California 92664
Attn: Library
Attn: G. Benford
Attn: N. Rynn

California Institute of Technology
Pasadena, California 91109
Attn: L. Davis, Jr.
Attn: P. Coleman

University of Chicago
Encrico Fermi Institute
Chicago, Illinois 60637
Attn: E. N. Parker
Attn: I. Lerche
Attn: Library

University of Colorado
Dept. of Astro-Geophysics
Boulder, Colorado 80302
Attn: M. Goldman
Attn: Library
Attn: D. Nicholson

Cornell University
Laboratory for Plasma Physics
Ithaca, New York 14850
Attn: Library
Attn: R. Sudan
Attn: D. Farley
Attn: T. Gold
Attn: F. Morse
Attn: R. Lovelace
Attn: M. Kelley

Columbia University
New York, New York 10027
Attn: R. Taussig
Attn: R. A. Gross

Harvard University
Cambridge, Massachusetts 02138
Attn: Harvard College Observatory (Library)
Attn: G. S. Vaina
Attn: M. Rosenberg

Harvard University
Center for Astrophysics
60 Garden St.
Cambridge, Mass. 02138
Attn: G. B. Field

University of Iowa
Iowa City, Iowa 52240
Attn: J. Van Allen
Attn: C. K. Goertz
Attn: G. Knorr
Attn: D. A. Gurnett
Attn: L. A. Frank

The John Hopkins University
Applied Physics Lab.
John Hopkins Rd.
Laurel, Maryland 20810
Attn: T. Krimigis
Attn: T. Potemra

John Hopkins University
Baltimore, Maryland 21218
Attn: Library
Attn: P. D. Feldman

University of Houston
Dept. of Physics
Houston, Texas 77004
Attn: Library
Attn: E. A. Bering

University of Michigan
Ann Arbor, Michigan 48104
Attn: E. Fontheim
Attn: L. Alvarez
Attn: A. Nagy
Attn: V. Bhatnagar

University of Minnesota
School of Physics
Minneapolis, Minn. 55455
Attn: Library
Attn: P. Kellogg
Attn: D. Cartwright
Attn: J. R. Winckler

M. I. T.
Cambridge, Massachusetts 02139
Attn: Library
Physics Dept. - Attn: B. Coppi
Attn: V. George
Elec. Engineering - Attn: R. Parker
Attn: A. Bers
Attn: L. Smullin
R. L. E. - Attn: Library
Space Science - Attn: Reading Room

University of New Hampshire
Durham, New Hampshire 03824
Attn: R. L. Arnoldy

Northwestern University
Evanston, Illinois 60201
Attn: J. Denevit

Princeton University
Princeton, New Jersey 08540
Attn: Physics Library
Attn: Plasma Physics Laboratory Library
Attn: C. Oberman
Attn: F. Perkins
Attn: R. White
Attn: R. Kurlsrud

Rice University
Houston, Texas 77001
Attn: Space Science Library
Attn: J. Chamberlain
Attn: R. Wolf
Attn: H. R. Anderson
Attn: A. Dessler

University of Rochester
Rochester, New York 10627
Attn: A. Simon

Stanford University
Institute for Plasma Research
Stanford, California 94305
Attn: Library
Attn: F. W. Crawford

Stevens Institute of Technology
Hoboken, New Jersey 07030
Attn: G. Schmidt

University of Texas
Austin, Texas 78712
Attn: W. Drummond
Attn: W. Horton
Attn: D. Choi
Attn: R. Richardson
Attn: G. Leifeste

Austin Research Assoc.
600 W. 28th Street
Austin, Texas 78705
Attn: L. Sloan

Bell Laboratories
Murray Hill, New Jersey 07974
Attn: A. Hasegawa
Attn: L. Lanzerotti

Lockheed Research Laboratory
Palo Alto, California 94304
Attn: M. Walt
Attn: J. Cladis

Maxwell Laboratories
9244 Balboa Ave.
San Diego, Calif. 92123
Attn: A. Kolb

Physics International Co.
2400 Merced Street
San Leandro, California 94577
Attn: S. Putnam
Attn: T. Young

Science Applications Inc.
Lab. of Applied Plasma Studies
P.O. Box 2351
LaJolla, California 92037
Attn: N. Krall
Attn: L. Linson

TRW Systems Group
Space Sc. Dept.
One Space Park
Redondo Beach, California 90278
Attn: R. Fredericks
Attn: F. Scarf
Attn: G. Greenstadt

Space Sciences Laboratory
Lockheed Corp.
Palo Alto, California 94304
Attn: R. G. Johnson
Attn: R. D. Sharp
Attn: E. G. Shelley

Dr. Henry Mullaney
Code 427
O.N.R.
Arlington, Va. 22217

University of Washington
Seattle, Washington 98195
Attn: G. Parks
Attn: S. Kaye

College of William and Mary
Williamsburg, Virginia 23185
Attn: F. Crownfield

Aerospace Corporation
El Secundo, California 90009
Attn: F. Morse
Attn: M. Schulz

Amos Research Center
Moffet Field, California 94035
Attn: A. Barnes (Code N245-3)

Lawrence Livermore Laboratory
University of California
Livermore, California 94551
Attn: Library
Attn: J. DeGroot
Attn: R. Briggs
Attn: D. Pearlstein

Los Alamos Scientific Laboratory
P.O. Box 1663
Los Alamos, New Mexico 87344
Attn: Library
Attn: D. Forslund
Attn: J. Kindell
Attn: B. Bezzerides
Attn: H. Dreicer
Attn: L. Thode
Attn: B. Godfrey
Attn: W. Feldman

NOAA
325 Broadway St.
Boulder, Colorado 80302
Attn: J. Weinstock
Attn: Thomas Moore (SEL, R-43)
Attn: W. Bernstein
Attn: D. Williams
Attn: B. B. Balsley
Attn: D. Evans

Sandia Laboratories
Albuquerque, New Mexico 87115
Attn: T. Wright

Goddard Space Flight Center
Greenbelt, Md. 20771
Attn: Dr. D. Stern
Attn: Dr. R. Weber
Attn: Dr. J. Novaco
Attn: Dr. J. Fainberg
Attn: Dr. R. Fitzenreiter
Attn: Dr. M. Goldstein
Attn: Dr. R. Stone
Attn: Dr. T. Northrop

National Science Foundation
Atmosph. Res. Section (ST)
Washington, D.C. 20550
Attn: Dr. D. Peacock

John Hopkins University
Applied Physics Lab.
Laurel, Maryland 20810
Attn: E. C. Roelof
Attn: E. P. Keath

Jet Propulsion Laboratory
Pasadena, California 91103
Attn: B. Tsurutani
Attn: D. Chenete
Attn: E. Smith

N.A.S.A. Headquarters
Code ST
Washington, D.C. 20546
Attn: H. Glaser
Attn: D. Caufmann
Attn: I. Smerling

Advanced Research Projects Agency (ARPA)
Strategic Technology Office
Arlington, Virginia
Attn: Capt. Donald M. LeVine

Naval Research Laboratory
Washington, D.C. 20375
Attn: P. Mange
Attn: E. Peterkin
Attn: R. Meier
Attn: E. Szuszczewicz - Code 6127
Attn: T. Coffey - Code 6700 (20 copies)
Attn: J. P. Boris - Code 6750 (100 copies)

Director of Space & Environmental Laboratory
NOAA
Boulder, Colorado 80302
Attn: A. Glenn Jean
Attn: G. W. Adams
Attn: D. N. Anderson
Attn: K. Davies
Attn: R. F. Donnelly

Stanford Research Institute
333 Ravenswood Avenue
Menlo Park, CA 94025
ATTN: M. Baron
ATTN: L. L. Cobb
ATTN: Walter G. Chestnut
ATTN: David A. Johnson
ATTN: Charles L. Rino
ATTN: E. J. Fremouw
ATTN: Ray L. Leadabrand
ATTN: Donald Neilson

Stanford Research Institute
306 Wynn Drive, N. W.
Huntsville, AL 35805
ATTN: Dale H. Davis

Technology International Corporation
75 Wiggins Avenue
Bedford, MA 01730
ATTN: W. P. Boquist

TRW Systems Group
One Space Park
Redondo Beach, CA 90278
ATTN: P. H. Katsos
ATTN: J. W. Lowery

Utah State University
Contract/Grant Office
Logan, UT 84322
ATTN: Security Officer

Visidyne, Inc.
19 Third Avenue
North West Industrial Park
Burlington, MA 01803
ATTN: William Reidy
ATTN: Oscar Manley
ATTN: J. W. Carpenter